



HAL
open science

Study of the pseudobinary compounds $\text{LaNi}_{5-x}\text{Fe}_x$ ($x \leq 1.2$) by X-ray diffraction, Mössbauer spectroscopy and magnetic measurements

J. Lamloumi, A. Percheron-Guegan, J.C. Achard, G. Jehanno, D. Givord

► To cite this version:

J. Lamloumi, A. Percheron-Guegan, J.C. Achard, G. Jehanno, D. Givord. Study of the pseudobinary compounds $\text{LaNi}_{5-x}\text{Fe}_x$ ($x \leq 1.2$) by X-ray diffraction, Mössbauer spectroscopy and magnetic measurements. *Journal de Physique*, 1984, 45 (10), pp.1643-1652. 10.1051/jphys:0198400450100164300 . jpa-00209905

HAL Id: jpa-00209905

<https://hal.science/jpa-00209905>

Submitted on 4 Feb 2008

HAL is a multi-disciplinary open access archive for the deposit and dissemination of scientific research documents, whether they are published or not. The documents may come from teaching and research institutions in France or abroad, or from public or private research centers.

L'archive ouverte pluridisciplinaire **HAL**, est destinée au dépôt et à la diffusion de documents scientifiques de niveau recherche, publiés ou non, émanant des établissements d'enseignement et de recherche français ou étrangers, des laboratoires publics ou privés.

Classification
 Physics Abstracts
 75.30C

Study of the pseudobinary compounds $\text{LaNi}_{5-x}\text{Fe}_x$ ($x \leq 1.2$) by X-ray diffraction, Mössbauer spectroscopy and magnetic measurements

J. Lamloumi (+), A. Percheron-Guegan, J. C. Achard, G. Jehanno (*) and D. Givord (**)

Chimie Métallurgique des Terres Rares, C.N.R.S., 1 Place A. Briand, 92190 Meudon-Bellevue, France

(*) DPh. SRM, C.E.N. Saclay, 91191 Gif sur Yvette Cedex, France

(**) Laboratoire Louis Néel, C.N.R.S., 166X, 38042 Grenoble Cedex, France

(Reçu le 29 février 1984, accepté le 25 mai 1984)

Résumé. — Les expériences Mössbauer sur $\text{LaNi}_{5-x}\text{Fe}_x$ ($x \leq 1,2$) indiquent que les atomes de fer se localisent presque exclusivement sur les sites 3g du groupe d'espace $\text{P6}/\text{m}$ mm. Lorsque la teneur en fer croît, les mesures de susceptibilité montrent que les composés évoluent entre le comportement d'un paramagnétique et celui d'un ferromagnétique en passant par un comportement de type verre de spin. Dans le cas de l'échantillon le plus riche en fer ($x = 1,2$), les moments magnétiques portés par les atomes de fer s'orientent suivant l'axe c . La comparaison des mesures d'aimantation aux résultats Mössbauer laisse à penser que la substitution de fer au nickel induit un moment magnétique sur les atomes de nickel, non magnétique dans LaNi_5 .

Abstract. — Mössbauer experiments show that in $\text{LaNi}_{5-x}\text{Fe}_x$ ($x \leq 1.2$), the iron atoms are almost exclusively located on the 3g sites of the $\text{P6}/\text{m}$ mm space group. Susceptibility measurements show that, with increasing iron concentration, these compounds change from paramagnetic to ferromagnetic passing through a spin glass like behaviour. For the iron richest compound ($x = 1.2$) the iron magnetic moments align along the c axis. Comparison of magnetization measurements and Mössbauer results indicates that the substitution of iron for nickel in LaNi_5 induces a magnetic moment on the previously non magnetic nickel atoms.

1. Introduction.

In a previous investigation [1] we reported on the magnetic properties of LaNi_4Fe which exhibits a behaviour close to ferromagnetic with a magnetic moment too high to be ascribed only to the Fe moments. In comparison LaNi_5 is a Pauli paramagnet, the nickel is not magnetic and there is no evidence of any magnetic ordering [2].

In the present study we report on the localization of iron atoms in the hexagonal CaCu_5 type structure of LaNi_4Fe as determined by Mössbauer spectroscopy and on the magnetic behaviour of the series $\text{LaNi}_{5-x}\text{Fe}_x$ when the nickel atoms are gradually replaced by Fe atoms as determined by high field magnetization, low field susceptibility and Mössbauer measurements.

2. Experiment:

Polycrystalline samples of different iron contents were prepared by induction melting of the pure constituents (La : 99.9 %; Ni : 99.99 %; Fe : 99.99 %) under vacuum in a water cooled copper crucible. To ensure homogeneity and to avoid extra-phases, at least seven meltings followed by an annealing in vacuum for seven days at 1 100 °C are required. The composition and homogeneity of the compounds were checked by metallographic examination and microprobe analysis. For $x < 1$, the samples are quite homogeneous; for higher iron concentrations, in spite of the careful preparation, micrographic examination and microprobe analysis show there are small amounts (≈ 1 %) of an extra-phase (Fe_2Ni) undetectable by X-ray diffraction. Details have been given elsewhere [3]. The structure and the values of the lattice parameters were determined by X-ray diffraction. The low field susceptibility was measured using a SQUID magnetometer, set up by G. Fillion (laboratoire Louis Néel, Grenoble), between 10 and 300 K. The measurement

(+) Permanent address : Ecole Normale Supérieure de l'Enseignement Technique (E.N.S.E.T.), 5, Avenue Taha Houssein, 1008 Tunis, Tunisie.

precision is $\pm 10^{-5}$ e.m.u. Magnetization measurements were made at the S.N.C.I. (Grenoble) by an extraction method in applied field up to 150 kOe and between 4.2 and 300 K. For both the magnetic and susceptibility measurements, the samples were in the form of small pieces of ingot with masses in the range 100-300 mg. The Mössbauer spectra were obtained with a ^{57}Co in Rh source, the drive was operated in the constant acceleration, triangular velocity mode; the absorber contained between 4 and 5 mg of natural iron per cm^2 . The data was fitted by assuming Lorentzian line shapes using a program elaborated by Teillet and Varret [4].

3. Results.

3.1 X-RAY DIFFRACTION RESULTS AND Fe LOCALIZATION USING THE MÖSSBAUER EFFECT. — The X-ray diffraction diagrams, for all the samples ($0.25 \leq x \leq 1.2$) are consistent with a hexagonal phase. The lattice parameters increase linearly with increasing iron concentration (Fig. 1), and follow the relations :

$$a = 5.016 + 0.037 x \text{ \AA}$$

$$c = 3.985 + 0.033 x \text{ \AA}.$$

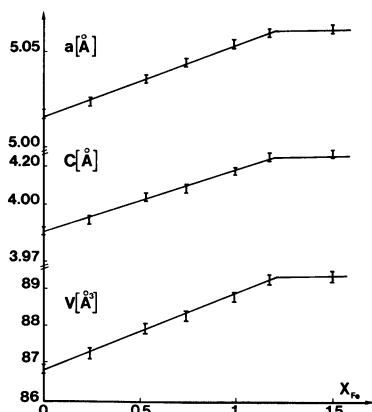


Fig. 1. — Variation of lattice parameters and cell volume as function of iron concentration.

It is known that LaNi_5 crystallizes in the CaCu_5 structure type (space group $\text{P6}/\text{m}\text{mm}$) [5]. X-ray examination of a small single crystal fragment taken from the polycrystalline ingot showed that LaNi_4Fe also crystallizes in the same structure. The intensity measurements agree very well with La being located at the 1a position, the other atoms being distributed over the 2c and 3g sites.

In order to determine the distribution of the iron atoms between the 2c and 3g sites, we used Mössbauer spectroscopy which is sensitive to the local symmetry of the sites. The two sites have different local symmetries : the 2c sites have axial symmetry ($\bar{6} \text{ m } 2$) whereas the 3g sites, situated at the intersection

of three twofold axes, have lower than axial symmetry. Thus, contrary to the 2c sites, the 3g sites are expected to show the influence of the asymmetry parameter (η) associated with the electric field gradient. The Mössbauer study was carried out on four samples with $x = 0.50, 0.75, 1.0$ and 1.2 .

In a previous study devoted to LaNi_4Fe [1], we interpreted the data in terms of a single type of site for the Fe (a similar result was obtained by Atzmony *et al.* [6]) with a well defined associated quadrupole splitting ($\Delta E_Q \sim 1.0 \text{ mm/s}$). A more careful examination of data taken at lower Doppler velocities ($V_{\text{max}} = 1.2 \text{ mm/s}$) shows that in all the samples there is in fact also present a second weak quadrupole doublet ($\Delta E_Q \sim 1.36 \text{ mm/s}$) (Fig. 2). This doublet has the same isomer shift as the main doublet and its relative intensity is near 5 %.

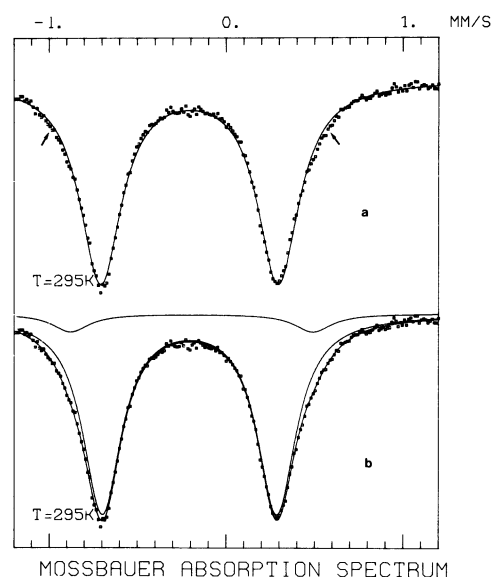


Fig. 2. — Room temperature Mössbauer spectrum for LaNi_4Fe . (a) : Fitting by a single doublet (arrows indicate some misfit). (b) : Fitting by two superimposed doublets.

The hyperfine parameters for the different samples in the paramagnetic region are given in table I. These values are very similar for all the samples, even for the samples without extra phase ($x \leq 0.75$), which led us to conclude that these two doublets are related to iron atoms on the two types of sites 2c and 3g. However we have to mention that the weak doublet is quite different from that observed by Campbell *et al.* [7] for a sample with $x = 0.25$, prepared in a different way but having received an annealing treatment similar to that given to our samples. These authors reported the presence of two quadrupole doublets with different quadrupole splittings ($\Delta E_Q \sim 1.0$ and 0.6 mm.s^{-1}) and with isomer shifts differing by $\sim 1.0 \text{ mm.s}^{-1}$. From their relative intensities, these two doublets were assigned to the two types of iron sites.

Table I. — *Hyperfine parameters of intermetallic LaNi_{5-x}Fe_x compounds at room temperature. δ : isomer shift relativ to metallic iron at room temperature, ΔE_Q : quadrupole splitting = $\frac{1}{2}eq^2 Q \sqrt{1 + \frac{\eta^2}{3}}$, Γ : half line-widths.*

x	T (K)	δ (mm/s)	ΔE_Q (mm/s)	Γ (mm/s)	%
0.5	295	- 0.109/- 0.086	0.987/1.428	0.266/0.266	94/6
0.75	295	- 0.099/- 0.071	0.968/1.377	0.264/0.212	95/5
1.0	295	- 0.099/- 0.064	0.991/1.460	0.292/0.240	94/6
1.2	295	- 0.094/- 0.066	0.988/1.288	0.272/0.272	94/6

To establish the nature of the site responsible for the dominant doublet in our spectra, we considered the role of the asymmetry parameter η . Because only polycrystalline samples were available we were not able to use the method of Zory [8] which can provide evidence for existence of the asymmetry parameter from the data in the paramagnetic region. Consequently, to obtain information concerning the eventual existence of η , we used the Mössbauer data obtained on the sample with $x=1.2$ in the magnetically ordered region. As shown in figure 3a, the data fits obtained assuming $\eta = 0$ are inadequate in the central region (discrepancy concerning the intensities of the central lines and their separation). When η is fitted along with the other parameters (table II) a good data fit is obtained (Fig. 3b). This fit provides a quadrupole interaction which is compatible with that obtained in the paramagnetic region.

This evidence in favour of a non-zero asymmetry parameter (η) thus shows that the majority (95 %) of the Fe atoms occupy the 3g sites of the median plane. Let us note that in the LaNi_{5-x}M_x (with M = Al, Si, Mn, Cu), it was shown, from neutron diffraction experiments [9], that the M atoms preferentially occupy 3g sites and exclusively this site

in the case of Al and Si. For the isomorphous compound Th(Ni, Fe)₅ it was also concluded [10] that iron atoms predominantly occupy the 3g sites.

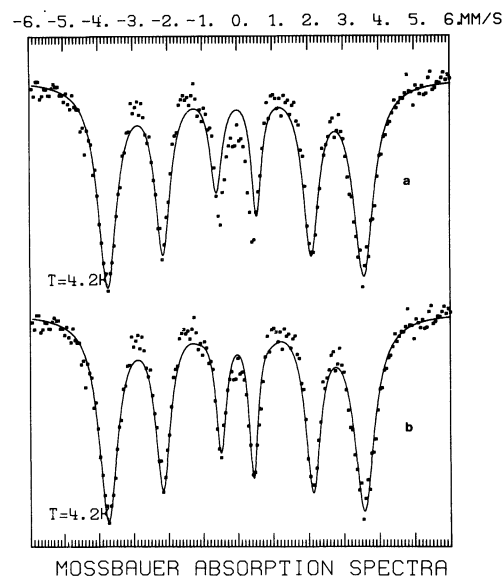


Fig. 3. — Mössbauer spectrum for LaNi_{3.8}Fe_{1.2} at $T = 4.2$ K ($\eta = 0$ (a); $\eta \neq 0$ (b)).

Table II. — LaNi_{3.8}Fe_{1.2} hyperfine parameters fitted with $\eta = 0$ and $\eta \neq 0$.

T (K)	η	ΔE_Q (mm/s)	δ (mm/s)	H_{hf} (kOe)	θ (degrés)
4.2	0*	- 0.07	0.034	227	25
4.2	0.78	1.16	0.034	220	78
77	0.8	1.14	0.034	201	81
77	0*	- 0.02	0.014	208	71
140	0.78	1.03	0.004	171	85
200	0.78	1.21	- 0.056	110	87

3.2 LOW FIELD d-c SUSCEPTIBILITY. — After cooling in zero magnetic field, the d-c susceptibility of the compounds was measured in a constant field for increasing (χ_c) and then decreasing (χ_d) temperature.

The temperature dependence of the susceptibility measured in an applied field of 3.5, 35, 100 and 1 000 Oe is shown in figures 4.1, 4.2, 4.3.

For the compound with the smallest iron concentration $\text{LaNi}_{4.75}\text{Fe}_{0.25}$, in a 35 Oe field, there is a monotonic decrease of the susceptibility above 110 K (Fig. 4.1). The weak hysteresis observed at lower temperatures could be due to magnetic inhomogeneity.

For $\text{LaNi}_{4.5}\text{Fe}_{0.5}$ and $\text{LaNi}_{4.25}\text{Fe}_{0.75}$ (Fig. 4.1), χ_c exhibits a pseudo peak at T_m . The amplitude of the peak is more pronounced when $x = 0.75$. Hysteresis effects appear below a temperature T_h different from T_m . The susceptibility is reversible above T_h but below T_h : $\chi_d > \chi_c$.

The influence of an applied field on the hysteresis effect was examined in the case of LaNi_4Fe (Fig. 4.2). The hysteresis effect, very important below $T_m = 190$ K, decreases with increasing field and disappears for an applied field = 1 000 Oe.

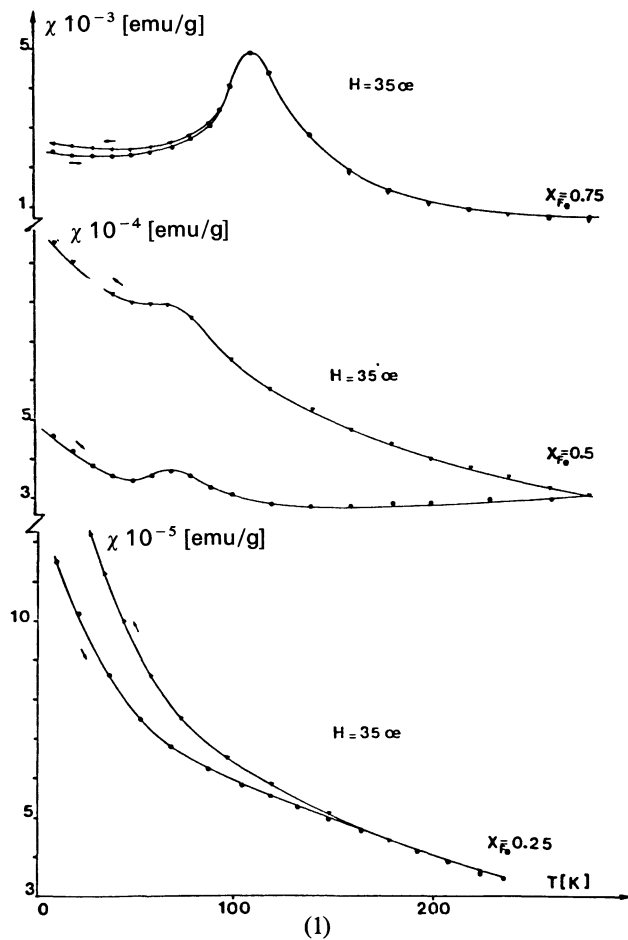
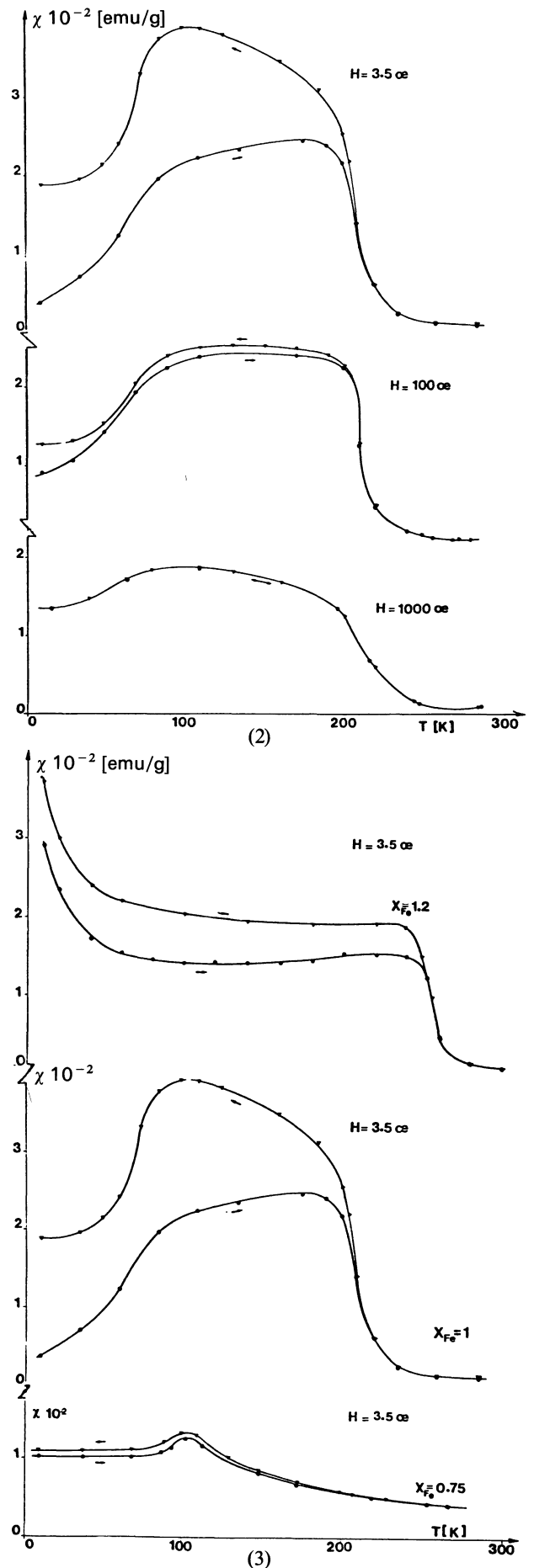


Fig. 4. — Magnetic susceptibility versus increasing (χ_c) and decreasing (χ_d) temperature for $\text{LaNi}_{5-x}\text{Fe}_x$.
 (1) : $x = 0.25$, $x = 0.5$, $x = 0.75$; applied field = 35 Oe.
 (2) : $x = 1$; several applied fields ($H = 3.5$ Oe, 100, 1 000 Oe).
 (3) : $x = 0.75$, $x = 1.0$, $x = 1.2$; applied field = 3.5 Oe.



Such behaviour of the susceptibility for these three compounds resembles that of spin-glass compounds.

The susceptibility of LaNi_{3.8}Fe_{1.2} in a 3.5 Oe field (Fig. 4.3) decreases above 10 K up to 80 K, then it becomes constant up to 240 K where it decreases abruptly. This behaviour is typical of a ferromagnetic compound undergoing a magnetic transition at $T_m = 240$ K.

3.3 MAGNETIZATION. — Magnetization curves were measured as a function of field between 4.2 K and 300 K in fields up to 150 kOe. These measurements, give equilibrium values since, as we have shown previously, the susceptibility is reversible above 1 000 Oe. The results obtained for the different compounds are shown in figures 5 and 6. For $x = 0.25$, the magnetization remains weak over the whole range of field and temperature. At 4.2 K and 150 kOe the magnetization is not saturated, its value is 6.83 e.m.u/g ($0.53 \mu_B$ per formula unit). The variations of the magnetization as a function of field are linear above 40 K; below, a slight deviation is observed. For $x = 0.5$ the magnetization increases linearly in the field range, above 50 kOe, and at temperatures above 120 K. The saturation is not reached at 150 kOe and 4.2 K; the magnetization is equal to 17.43 e.m.u/g ($1.35 \mu_B$ per formula unit). For $x = 0.75$, the magnetization shows a stronger dependence on decreasing

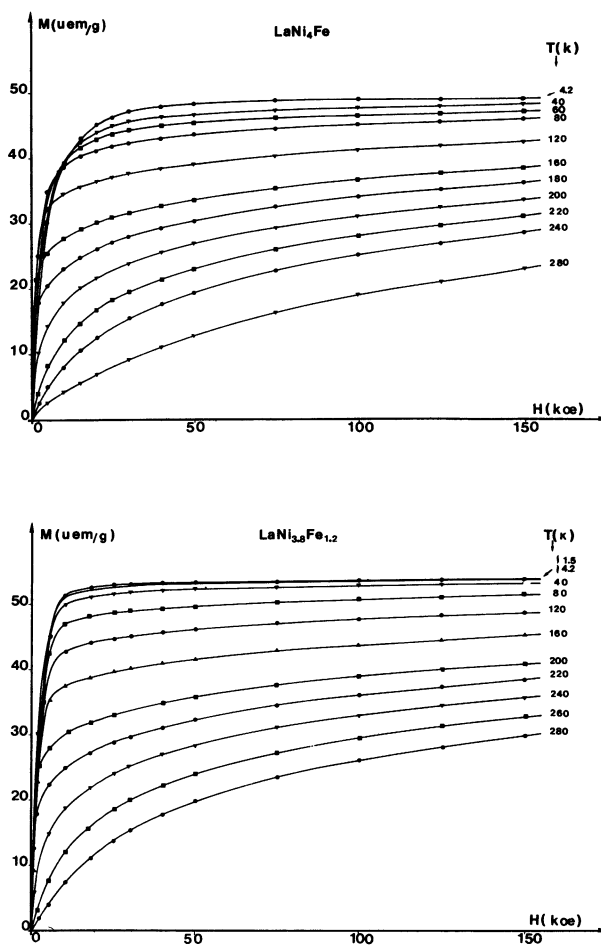


Fig. 6. — Magnetization (M) of LaNi₄Fe and LaNi_{3.8}Fe_{1.2} versus applied field (H) at different temperatures.

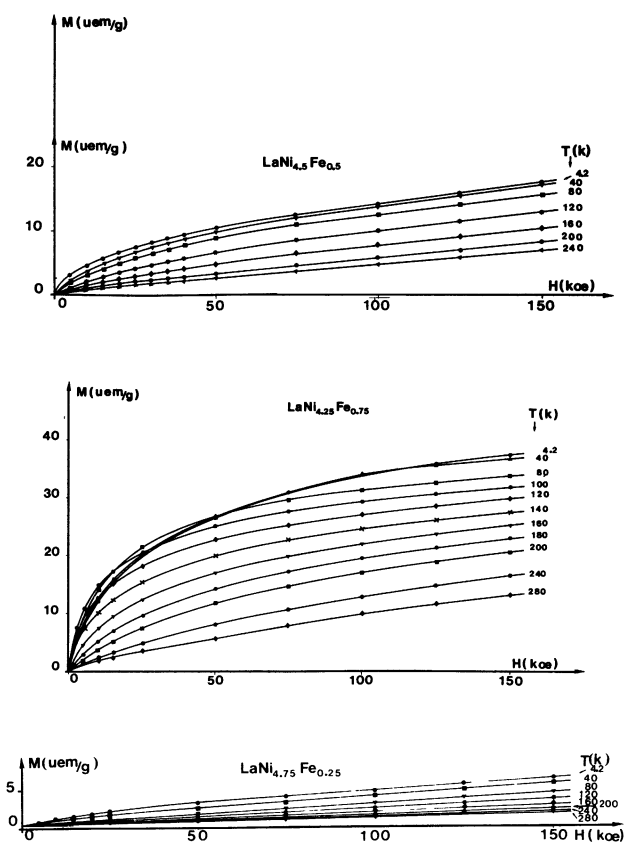


Fig. 5. — Magnetization (M) of LaNi_{5-x}Fe_x ($x = 0.25$, $x = 0.5$, $x = 0.75$) versus applied field (H) at different temperatures.

temperature and increasing field. For $x = 1.0$, the saturation is almost reached at 4.2 K and 150 kOe. From an extrapolation against $1/H$, the saturation magnetization, μ_s at 4.2 K is obtained ($3.9 \mu_B$ per formula unit). This value is in agreement with that previously determined [11]. The initial slope of the magnetization curves changes with temperature and at 4.2 K is less than that expected for a demagnetizing field ($H_d = 1.5$ kOe instead of 1.75 kOe). For $x = 1.2$ at low temperatures and for fields higher than 25 kOe, the saturation is reached. At 4.2 K, the saturation magnetization obtained as in the previous case is $\mu_s = 4.18 \mu_B$ per formula unit. The initial slope of the magnetization curves is temperature independent, its value, equal to 1.95 kOe, is essentially equal to that of the demagnetizing field $H_d = 2$ kOe. These properties are typical of a ferromagnetic behaviour. The main results obtained from these measurements are summarized in tables IIIa and IIIb.

3.4 MÖSSBAUER MEASUREMENTS.

3.4.1 Magnetic transition temperatures. — The ordering temperatures cannot be obtained exactly using Mössbauer spectroscopy because the absorption line

Table IIIa. — Values, as function of the iron concentration, of : the temperatures of maximum of the susceptibility (χ_c) for $0.5 \leq x \leq 1$ and of the magnetic transition for $x = 1.2$; the Mössbauer transition temperature : T_t ; the hysteresis temperature : T_h ; the magnetization M at $T = 4.2$ K, applied field = 150 kOe; the saturated moment (magnetization results) : μ_s ; the magnetic moment (Mössbauer results) : m .

x	0.25	0.5	0.75	1	1.2
T_m (K)	—	$\simeq 70$	110	190	240
T_t (K)	—	~ 50	95	190	~ 235
T_h (K)	—	> 300	$\simeq 200$	230	240
M (150 kOe, 4.2 K) (μ_B /Formule)	0.53	1.35	2.87	3.79	4.15
μ_s (μ_B /Formule)	—	—	3.5	3.88	4.18
m (μ_B /Fe)	—	1.23	1.41	1.49	1.52

Table IIIb. — Effective magnetic moments, paramagnetic Curie temperature and temperatures deduced from the Arrott plots as function of iron concentration.

x	0.25	0.5	0.75	1	1.2
μ_{eff} (μ_B /Formule)	5.9	19.3	20.6	15.7	10.7
T_c (K) paramagnetic	< 0	< 0	95	200	260
T_{Arrott} (K)	—	—	155	240	—

shapes only change relatively gradually with temperature. This is particularly the case for the samples with $x = 0.5$ and 0.75 for which the magnetic spectra have not been exploited in detail. An example of the thermal evolution of the absorption for LaNi_4Fe is given in figure 7. As is shown in figure 8, the ordering temperature increases progressively with increasing iron content from $\simeq 50$ K for $x = 0.75$ to $\simeq 235$ K for $x = 1.2$.

3.4.2 *Magnetic moments on the Fe atoms.* — The hyperfine field, measured at 4.2 K, as a function of x is shown on figure 9a. The field increases with x to reach a value of 220 kOe for $x = 1.2$. Using the relationship between iron moment and hyperfine field that has been established for metallic iron ($1 \mu_B \rightarrow 145$ kOe), we have calculated the Fe atomic moments and these are given in table IIIa. We can note that the thermal evolution of the hyperfine field is more gradual for $x = 1.0$ than for $x = 1.2$ (Fig. 9b).

3.4.3 *Magnetic moment orientations.* — The orientations of the magnetic moments relative to the crystal axis have been determined for the samples $x = 1.0$ and $x = 1.2$, that is for the cases where the best resolv-

ed hyperfine structure we observed. In the data fits only the dominant site (3g) was taken into account. The fitted parameter were the same whether or not the weakly populated (2c) sites were included in the analysis.

The fitting procedure was carried out using independent line-widths for the different components. This takes into account a possible distribution in size of the hyperfine field and a possible distribution in θ , the angle between this field and the principal axis of the electrical field gradient (E.F.G.).

For $x = 1.2$, at all temperatures down to 4.2 K, and for $x = 1.0$ for all temperatures down to 100 K, the data fits show that θ is close to 90° and that η is high (0.7 to 0.8) (Table IV).

For $x = 1.0$ the analysis of the data below 100 K indicates that θ varies with temperature. This result will be considered in more detail elsewhere [12].

In this context we can note that our point charge calculation in terms of Ni^{2+} and La^{3+} shows that the principal axis of E.F.G. ($V_{zz} > 0$) lies along the twofold axis $\langle 1\bar{1}0 \rangle$ and the component with the smallest absolute value (V_{xx}) lies along the crystal c -axis, this qualitative result, together with the value

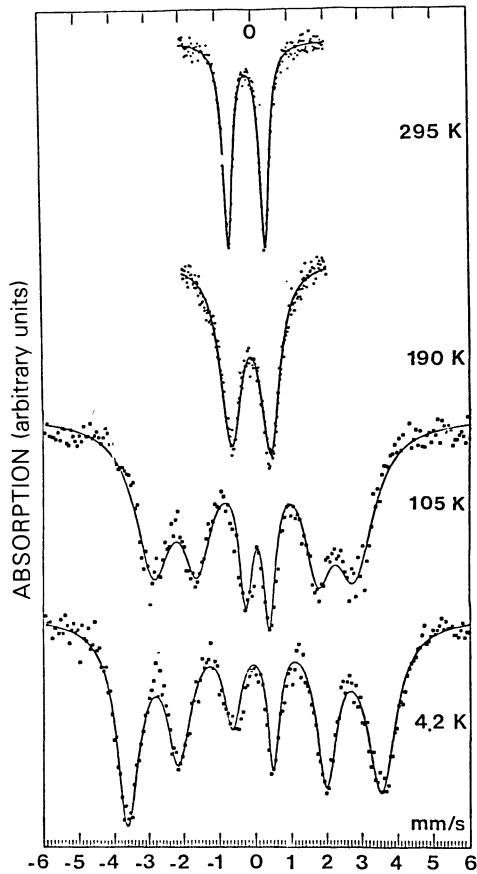


Fig. 7. — Mössbauer spectra of LaNi₄Fe at different temperatures.

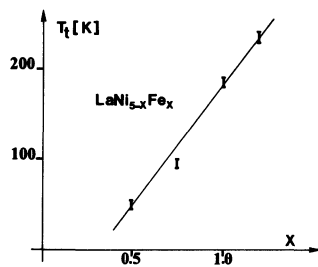


Fig. 8. — Magnetic transition temperatures (Mössbauer results) for LaNi_{5-x}Fe_x (0.5 ≤ x ≤ 1.2).

$\theta = 90^\circ$ deduced above, indicates that the Fe moments are aligned parallel to the \bar{c} axis, the only axis which is perpendicular to the three distinct and coplanar principal axes of the E.F.G. at the 3g sites. This point was confirmed by joint experiments involving Mössbauer absorption in a magnetic field and X-ray diffraction after applying a field.

It is known that when a magnetic field sufficiently strong to align the magnetic moments, is applied parallel to the γ -ray axis then the $\Delta m = 0$ transitions are suppressed and the other transitions are broadened when a quadrupole interaction is present. This is what is observed here at 4.2 K in a field of 50 kOe, when the powder making up the sample was immo-

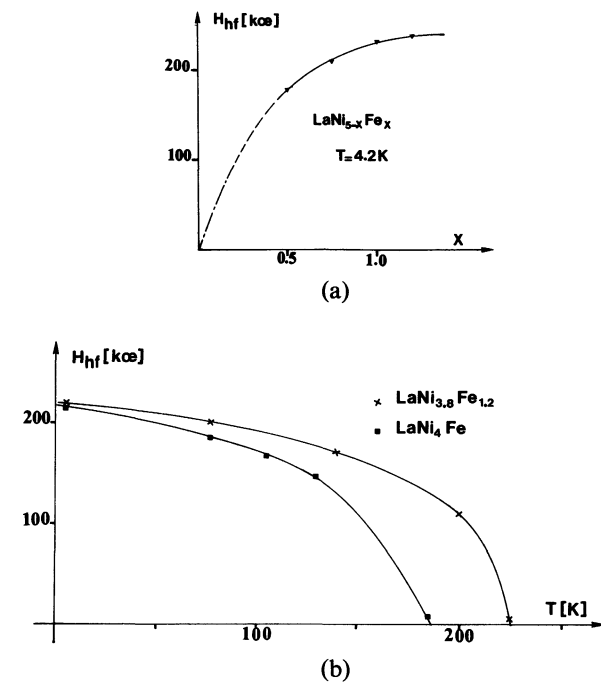


Fig. 9. — (a) : Hyperfine field (H_{hf}) for LaNi_{5-x}Fe_x (0.5 ≤ x ≤ 1.2) at $T = 4.2$ K. (b) : Hyperfine field versus temperature for LaNi₄Fe and LaNi_{3.8}Fe_{1.2}.

bilized by surrounding it by an epoxy resin. However using the same procedure but allowing the grains to freely rotate produces the absorption pattern shown in figure 10. Here the individual components are sharper than for the absorption pattern obtained in absence of a magnetic field. This result shows that with the grains free to move, the magnetic moments become completely aligned with the applied magnetic field at the same time that the grains undergo reorien-

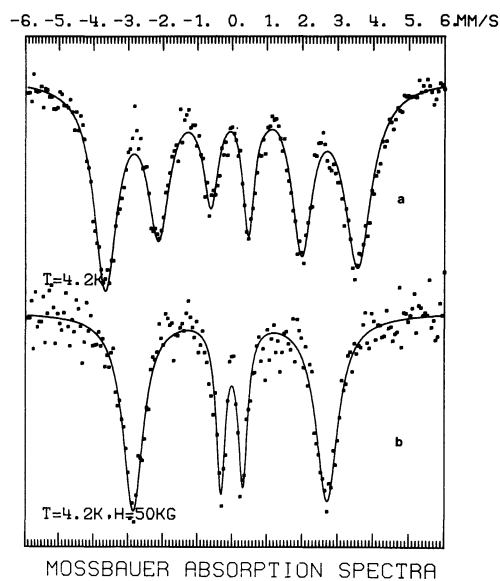


Fig. 10. — Mössbauer spectra for LaNi₄Fe at $T = 4.2$ K, (a) : without applied field, (b) : under field ($H = 50$ kOe) parallel to γ radiation.

Table IV. — *Hyperfine parameters, angle θ between the hyperfine field and the principal axis oz of E.F.G., asymmetry parameter η of E.F.G. versus iron concentration. (* means that the corresponding parameter values are imposed during the fitting procedure.)*

x	T (K)	δ mm/s	ΔE_Q mm/s	H_{hf} (kOe)	θ (degré)	η
0.5	4.2	0.004	1.44	179	61	0.74
0.75	4.2	0.024	0.88	205	60	0.55
1.0	4.2	0.034	1.00	216	63	0.59
	77	0.034	1.00	185	74	0.71
	105	0.004	1.00	166	80	0.70
	105	0.004	1.00*	167	90*	0.76
	130	0.006	1.00*	145	78	0.67
	130	0.006	1.00	145	90*	0.7
	190	0.026	1.1	4.9	—	—
1.2	4.2	0.034	1.16	220	78	0.78
	4.2	0.034	1.07	221	90*	0.86
	77	0.034	1.14	201	81	0.80
	77	0.034	1.10	210	90*	0.86
	140	0.004	1.03	171	85*	0.78*
	140	0.014	1.03	171	90*	0.88
	200	-0.056	1.21	110	87	0.78

tations. The measured effective field is reduced by an amount equal to the applied field, which is consistent with the negative sign of the hyperfine field.

A preferential orientation of the grains as shown by room temperature X-ray diffraction has also been observed with a field of 25 kOe applied at 77 K ($T < T_i$) with the applied field either parallel or perpendicular to the surface plane of the total sample. The room temperature and zero field X-ray data are shown in figure 11.

For $x = 1.2$, after the field is applied perpendicular to the surface plane of the sample, figure 11b shows that the intensity of the (002) reflection increases and that the intensities of the (110) and (200) reflections decrease. This shows that the easy magnetization direction lies along the \bar{c} axis. After the field is applied parallel to the surface plane of the sample, the opposite effect is observed (Fig. 11c).

For $x = 1.0$, a similar behaviour is observed although it is less pronounced. This may be either a manifestation of a less important magnetic anisotropy or, alternatively, of the fact that at $T = 77$ K (the temperature of the sample when the field was applied) the moments are no longer aligned along the $\langle 001 \rangle$ direction as indicated by the change in θ obtained from the data fits for $T < 100$ K.

4. Discussion.

It is known that the LaNi_5 compound is a reinforced exchange Pauli paramagnetic with a temperature independent susceptibility [2].

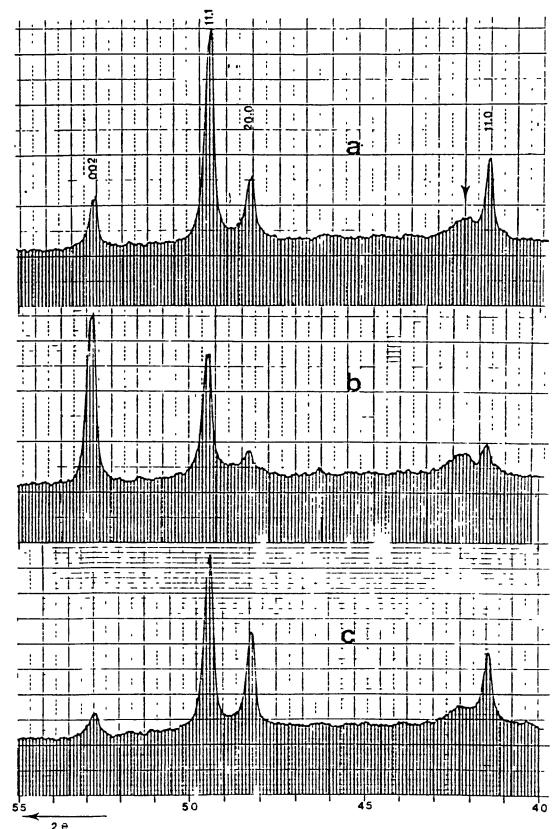


Fig. 11. — X-ray diffraction for $\text{LaNi}_{3.8}\text{Fe}_{1.2}$. (a) : Before applying magnetic field. (b) : Sample submitted to magnetic field ($H = 25$ kOe) perpendicular to its surface. (c) : Sample submitted to magnetic field ($H = 25$ kOe) parallel to its surface.

The substitution of 5 % Fe for Ni gives rise to a Curie-Weiss paramagnetic behaviour, since the reverse susceptibility varies linearly with increasing temperature.

For compounds with 0.5 ≤ x < 1, the thermal dependence of the susceptibility measured in a constant low field exhibits a pseudo peak at T_m and an hysteresis effect below T_h with χ_c < χ_d, which is typical of spin-glass systems.

In the ideal case these systems can be considered to be a collection of randomly distributed isolated moments frozen in random orientation in a non magnetic matrix. When the magnetic atom concentration increases, magnetic clusters, with giant moments, are created within the spin glass matrix.

In the present case, the thermal dependence of the reverse χ_d, above T_h, measured for 3.5 Oe and 35 Oe is almost linear and we can deduce the effective mean moment using a Curie-Weiss law (Table IIIb). The comparison of these high values for the various compositions to the value of the effective moments of Fe and Ni suggests the existence of magnetic clusters with giant moments. The size of the clusters would reach a maximum for x = 0.75.

For LaNi₄Fe, the disappearance of the interactions existing at low temperature between the frozen moments of the matrix and the giant moments as a function of increasing field, is illustrated (Fig. 4.2) by the progressive disappearance of the hysteresis effect.

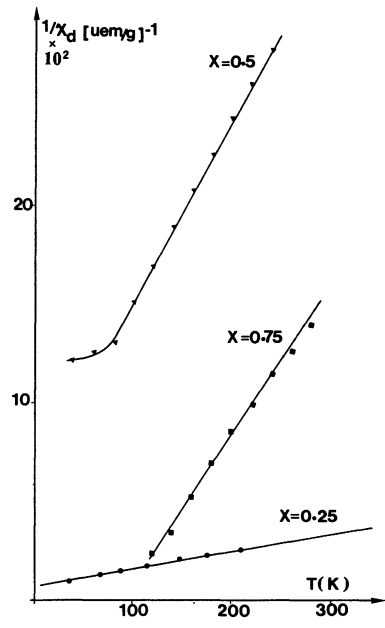
On the other hand, the paramagnetic Curie temperature deduced from the thermal dependence of the reverse susceptibility (Fig. 12) allows the interaction existing between the magnetic clusters to be defined.

The values summarized in the table III show that for x ≤ 0.5, the Curie temperatures are negative, which is a consequence of the predominance of negative interactions. For the richer iron compounds, Curie temperatures become positive showing the predominance of positive interactions between the clusters.

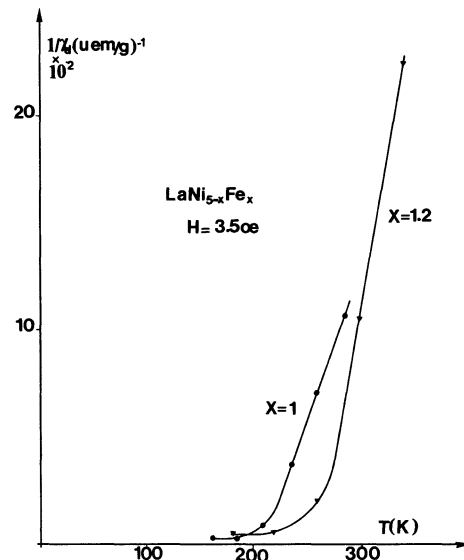
Arrott plots derived from the magnetization curves are linear only for high fields (H > 50 kOe). Extrapolating the high-field slope leads to ordering temperatures 155 K and 240 K respectively for x = 0.75 and x = 1.0. It is noticeable that these values are higher than those determined in zero field by Mössbauer effect, 110 K and 190 K respectively, which confirms the influence of the field on these interactions.

Finally for the richest iron compound LaNi_{3.8}Fe_{1.2}, the low field susceptibility is equal to the slope of the demagnetization field, the saturation magnetization is reached for low field, the direction of moments parallel to c is independent of field and temperature; this shows the preponderance of positive interactions between the magnetic clusters in this compound. The ordering temperature T_c around T = 240 K reflects the order of magnitude of the short range ferromagnetic order.

The comparison of the variation of the magnetiza-



(a)



(b)

Fig. 12. — Thermal variation of the reverse susceptibility for LaNi_{5-x}Fe_x compounds. (a) : x = 0.25, x = 0.5, x = 0.75, applied field = 35 Oe. (b) : x = 1.0, x = 1.2, applied field = 3.5 Oe.

tion as a function of applied field at 4.2 K for the different iron concentrations, gives some indication of the competition between positive and negative interactions. The magnetization of the compounds with less than 20 % iron shows field dependence and no saturation : the moments are not parallel.

For 24 % iron (x = 1.2) the behaviour is purely ferromagnetic. The properties of x = 0.75; x = 1 are nearly ferromagnetic with a progressive decrease of the negative interaction, dominant in the less iron rich alloys (x = 0.25).

This coexistence of positive and negative interactions is often observed in rare earth iron compounds [13,

14] for which the 3d iron band is quasi half full. The interactions are determined by the interatomic distances; negative interactions corresponding to the short distances oppose positive interactions between more distant atoms.

Bulk magnetization measurements provided a determination of μ_s , the average moment per formula, in strong magnetic fields. Mössbauer measurements give the hyperfine field in zero applied field from which the moment of the iron atoms only can be deduced. It has been observed that this moment remains the same under an applied field of 50 kOe (the effective field being only reduced by this amount). Comparison of the average moment obtained by the two methods (Fig. 13) shows that μ_s is always greater than μ_m , so that the magnetic contribution of nickel can be deduced.

We tried to estimate this contribution in the case of $\text{LaNi}_{3.8}\text{Fe}_{1.2}$, the only case where saturation magnetization is easily reached : $\mu_s = 4.18 \mu_B$.

Assuming for the iron moment the theoretical value of $2.2 \mu_B$, we get for nickel $0.4 \mu_B/\text{atom}$. If we take the experimental Mössbauer value, i.e. $1.52 \mu_B/\text{atom}$, we get $0.62 \mu_B/\text{atom Ni}$. We can then conclude that

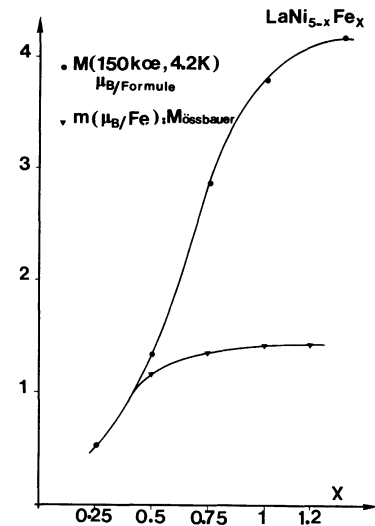


Fig. 13. — Magnetic moments : M (Magnetization results at $T = 4.2 \text{ K}$ and $H = 150 \text{ kOe}$) and m (Mössbauer results) for $\text{LaNi}_{5-x}\text{Fe}_x$ compounds.

Fe substitution for non magnetic nickel in LaNi_5 induces a moment on Ni atoms.

References

- [1] LAMLOUMI, J., LARTIGUE, C., PERCHERON-GUEGAN, A. and ACHARD, J. C., JEHANNO, G., *The Rare Earth in Modern Sciences and Technology* 3 (1982) 487.
- [2] PALLEAU, G., CHOUTEAU, G., *J. Physique Lett.* 41 (1980) L-227 and references herein.
- [3] LAMLOUMI, J., Thèse de 3^e cycle, Paris VI, 1982.
- [4] TEILLET, J., VARRET, F., Unpublished MOSFIT program.
- [5] WERNICK, J. H., GELLER, S., *Acta Cryst.* 12 (1959) 662.
- [6] ATZMONY, U., DAYAN, D. and DARIEL, M. P., *Mat. Res. Bull.* 16 (1981) 793-797.
- [7] CAMPBELL, S. J., DAY, R. K., *et al.*, *J. Mag. Mag. Mat.* 31-34 (1983) 167-168.
- [8] ZORY, P., *Phys. Rev.* 140 (1965) A 1401.
- [9] PERCHERON-GUEGAN, A., LARTIGUE, C., ACHARD, J. C., GERMI, P., TASSET, F., *J. Less Com. Met.* 74 (1980) 1.12 and *The Rare Earths in Modern Science and Technology* 3 (1982) 481 edited by McCarthy, Silber and Rhyne (Plenum Publishing Corporation).
- [10] ELEMANS, J. B. A. A. and BUSCHOW, K. H. J., *Phys. Status Solidi (a)* 34 (1976) 355.
- [11] ELEMANS, J. B. A. A., BUSCHOW, K. H. J., ZANDBERGEN, H. W. and DE JONG, J. P., *Phys. Status Solid (a)* 29 (1975) 595.
- [12] JEHANNO, G., LAMLOUMI, J., PERCHERON-GUEGAN, A. and ACHARD, J. C., to be published in *Solid State Commun.*
- [13] HEIMAN, N., KAZAMA, N., *Phys. Rev. B* 19 (1979) 1623.
- [14] GIVORD, D., LEMAIRE, R., *I.E.E.E. Trans. Mag. Mag.* 10 (1974) 109.